Author Manuscript

Author Manuscript

Author Manuscript

Author Manuscript

HHS Public Access

Author manuscript

*Neuroscience*. Author manuscript; available in PMC 2019 June 01.

Published in final edited form as:

*Neuroscience*. 2018 June 01; 380: 90–102. doi:10.1016/j.neuroscience.2018.04.004.

# $Ca^{2+}$ binding protein 1 regulates hippocampal-dependent memory and synaptic plasticity

**Tian Yang**[a], **Jeremiah K. Britt**[b], **Coral J. Cintrón-Pérez**[b], **Edwin Vázquez-Rosa**[b], **Kevin V. Tobin**[a], **Grant Stalker**[a], **Jason Hardie**[a], **Rebecca J. Taugher**[b], **John Wemmie**[b], **Andrew A Pieper**[b,c,d,e,f,g,h], and **Amy Lee**[a]

[a]Departments of Molecular Physiology and Biophysics, Otolaryngology Head-Neck Surgery, Neurology, University of Iowa, Iowa City, IA 52242, USA

[b]Department of Psychiatry, University of Iowa, Iowa City, IA 52242, USA

[c]Department of Neurology, University of Iowa, Iowa City, IA 52242, USA

[d]Department of Free Radical, University of Iowa, Iowa City, IA 52242, USA

[e]Department of Radiation Biology Program, University of Iowa, Iowa City, IA 52242, USA

[f]Department of Radiation Oncology Comprehensive Cancer Center, University of Iowa, Iowa City, IA 52242, USA

[g]Department of Veterans Affairs, University of Iowa, Iowa City, IA 52242, USA

[h]Pappajohn Biomedical Institute and Iowa Neuroscience Institute, University of Iowa, Iowa City, IA 52242, USA

## Abstract

$Ca^{2+}$ binding protein 1 (CaBP1) is a $Ca^{2+}$ sensing protein similar to calmodulin that potently regulates voltage-gated $Ca^{2+}$ channels. Unlike calmodulin, however, CaBP1 is mainly expressed in neuronal cell-types and enriched in the hippocampus, where its function is unknown. Here, we investigated the role of CaBP1 in hippocampal-dependent behaviors using mice lacking expression of CaBP1 (C-KO). By western blot, the largest CaBP1 splice variant, caldendrin, was detected in hippocampal lysates from wild-type (WT) but not C-KO mice. Compared to WT mice, C-KO mice exhibited mild deficits in spatial learning and memory in both the Barnes maze and in Morris water maze reversal learning. In contextual but not cued fear conditioning assays, C-KO mice showed greater freezing responses than WT mice. In addition, the number of adult-born neurons in the hippocampus of C-KO mice was ~40% of that in WT mice, as measured by bromodeoxyuridine labeling. Moreover, hippocampal long-term potentiation was significantly reduced in C-KO mice. We conclude that CaBP1 is required for cellular mechanisms underlying optimal encoding of hippocampal-dependent spatial and fear-related memories.

Corresponding author: Amy Lee, Dept. of Molecular Physiology and Biophysics, University of Iowa, PBDB 5318, 169 Newton Road, Iowa City, IA 52242, Phone: (319) 384-1762, Fax: (319) 335-7330, amy-lee@uiowa.edu.

**Publisher's Disclaimer:** This is a PDF file of an unedited manuscript that has been accepted for publication. As a service to our customers we are providing this early version of the manuscript. The manuscript will undergo copyediting, typesetting, and review of the resulting proof before it is published in its final citable form. Please note that during the production process errors may be discovered which could affect the content, and all legal disclaimers that apply to the journal pertain.

Author Manuscript Author Manuscript Author Manuscript Author Manuscript

**Keywords**

calmodulin; synaptic plasticity; fear learning; memory; $Ca^{2+}$; hippocampus

## Introduction

$Ca^{2+}$ sensing proteins, such as calmodulin (CaM), play a central role in encoding and decoding neuronal $Ca^{2+}$ signaling. As the primordial member of a superfamily of $Ca^{2+}$ binding proteins (CaBPs) containing one or more EF-hand $Ca^{2+}$ binding domains (Kawasaki and Kretsinger, 2017), CaM binds to and regulates numerous enzymes (Hell, 2014), transcription factors (Finkler et al., 2007), and ion channels (Saimi and Kung, 2002). While CaM is widely expressed in most eukaryotic cell-types, a subset of these EF-hand proteins is also found primarily in neurons (Burgoyne and Haynes, 2012). These include hippocalcin and neuronal $Ca^{2+}$ sensor 1, which regulate long-term depression (Palmer et al., 2005) and spatial memory, respectively (Saab et al., 2009). By interacting with and modulating distinct effectors, these neuron-specific $Ca^{2+}$ binding proteins facilitate development and function of the nervous system by diversifying the $Ca^{2+}$ signaling repertoire in neurons.

Of all the neuron-specific $Ca^{2+}$ binding proteins, CaBPs are the subfamily that shares the most sequence homology with CaM (Haeseleer et al., 2000). Like CaM, CaBPs have 4 EF-hand domains, but with one of them harboring an amino acid substitution that prevents $Ca^{2+}$ binding (Haeseleer et al., 2002) (Fig.1A). Some CaBPs are highly expressed in retina, where they regulate photoreceptor synapse morphology and transmission (Haeseleer et al., 2004, Liu et al., 2013), as well as retinal ganglion cell responses to light (Rieke et al., 2008, Sinha et al., 2016). CaBPs are also expressed in the cochlea (Cui et al., 2007, Yang et al., 2016), where they regulate the function of inner hair cells in sound coding (Schrauwen et al., 2012, Picher et al., 2017).

CaBP1 is a CaBP family member that is not only expressed in the retina and inner ear, but also at high levels in the brain (Laube et al., 2002, Cui et al., 2007, Kim et al., 2014, Yang et al., 2016). Alternative splicing gives rise to multiple CaBP1 variants that differ in their N-terminal regions. Of these, caldendrin is most abundant in the brain (Laube et al., 2002, Kim et al., 2014). CaBP1 can compete with CaM for binding and regulating voltage-gated $Ca^{2+}$ channels (Hardie and Lee, 2016), and also strongly inhibits $Ca_v2.1$ P/Q-type channels by inhibiting their activation and enhancing their inactivation (Lee et al., 2002). By contrast, CaBP1 potentiates $Ca_v1$ L-type channels by suppressing their $Ca^{2+}$-dependent inactivation (Zhou et al., 2004, Zhou et al., 2005). Although the mechanisms underlying CaBP1 regulation of $Ca^{2+}$ channels have been explored in great detail in heterologous expression systems (Findeisen and Minor, 2010, Oz et al., 2013), the function of CaBP1 in the brain remains unknown.

To fill this gap, we analyzed behavioral alterations in mice lacking expression of all CaBP1 variants (C-KO; (Kim et al., 2014)). Because of the high expression of CaBP1 in hippocampus, we focused on hippocampal-dependent tasks (Laube et al., 2002, Kim et al., 2014). We show that C-KO mice exhibit alterations in spatial learning and memory, fear conditioning, survival of adult-born neurons, and synaptic plasticity. Our findings provide

Author Manuscript Author Manuscript Author Manuscript Author Manuscript

the first evidence for a role for CaBP1 in regulating information processing in the hippocampus, possibly through regulation of voltage-gated $Ca^{2+}$ channels and/or other targets.

## Experimental Procedures

### Animals

All experiments were performed in accordance with guidelines set by the Office of the Institutional Animal Care and Use Committee at the University of Iowa. The procedures used in this study are not expected to produce pain or suffering in the animals. Generation of C-KO mice was described previously (Kim et al., 2014). Mice were maintained on a C57BL/6N (Envigo) background and housed in groups on a standard 12:12 hour light: dark cycle, with food and water provided ad libitum. For behavioral tests and adult-born neuron assays, both males and females from 10 to 18 weeks were used. The data obtained for males and females was combined only after confirming there were no significant sex-specific differences. Otherwise, the data from males and females used were analyzed separately. Males from 2–4 months old were used for electrophysiology experiments. A total of 504 (252 WT and 252 KO) mice were used in this study.

### Western blotting

For preparation of hippocampal lysates, 10–16 week old WT (n = 12) and C-KO (n = 12) mice were anesthetized with isofluorane. Hippocampi were dissected in cold 1X PBS, and homogenized in CelLytic MT buffer (Sigma) supplemented with protease inhibitors. Tissues were collected by centrifuging at 100,000 × *g* for 30 min at 4°C. The pellet was resuspended and sonicated in binding buffer (50 mM Tris-HCl, 150 mM NaCl, 10 mM $CaCl_2$, pH 7.3). Samples were incubated for 30 min at 4°C, and then centrifuged at 10,000 × *g* for 10 min at 4°C. The supernatant was collected, and protein concentration was quantified using BCA Protein Assay Kit (Thermo Scientific Pierce) to ensure equal loading of protein for western blots. Each sample was prepared from hippocampi collected from 2 males and 2 females. Hippocampal lysates were then incubated with 4X SDS buffer supplemented with DTT (20 mM) at 60 °C for 10 min.

Protein samples were loaded into NuPage Novex 4–12% Bis–Tris gels for electrophoresis and transfer to a nitrocellulose membrane (BioRad, Hercules, CA, USA). The membrane was blocked for 1 h at room temperature (RT) in blocking buffer (BB: 5% milk in 1X TBST [50 mM Tris, 150 mM NaCl, 0.1% Tween 20, pH 7.4]). Blots were then incubated with antibodies against CaBP1 (UW72, 1:1000 diluted in BB; (Haeseleer et al., 2000)) for 1 h at RT, and then secondary donkey anti-rabbit horseradish peroxidase antibodies (1:4000 diluted in BB; GE Healthcare Cat# NA934, RRID:AB_772206) for 45 min at RT. The blot was rinsed with TBST between and after the antibody incubations. Western blot signals were visualized by incubating in chemiluminescence reagents (SuperSignal West Pico Chemiluminescent Substrate, Thermo Scientific) and exposing to autoradiography film.

Author Manuscript Author Manuscript Author Manuscript Author Manuscript

### Barnes maze test

Barnes maze was performed as described previously (Yin et al., 2014). The testing apparatus consisted of a 91-cm gray circular surface with 20 holes (5 cm in diameter) equally spaced around the perimeter (Stoelting). The surface was raised to a height of 90 cm under brightly lit and open conditions, and a dark escape chamber was put under one of the 20 holes. A black circular curtain with four different and equally spaced visual cues was hung around the circular surface to provide orientation to the mice. The training was performed over 4 days with 4 trials per day. A trial ended when the mouse entered the escape chamber or when the allowed testing time (80 s) ended. Mice that did not find the platform were guided to the escape hole. A probe trial of 60 sec was conducted on day 5, during which the escape chamber was removed. Measurements were acquired with Anymaze video tracking software (Stoelting). 54 WT (25 M and 29 F) and 52 C-KO (26 M and 26 F) mice were used.

### Morris water maze test

Morris water maze testing was conducted as described (Vorhees and Williams, 2006). A circular pool 4 ft in diameter was filled with room temperature water made opaque with white paint (Stoelting). The pool was surrounded by a black curtain, and 4 posters of different colors and shapes were hung on the curtain to serve as visual cues. During each training day, mice were put in one of four starting locations facing the pool wall and allowed to swim for 1 min. A trial ended when the mouse reached a visible platform or when the time ran out. At the end of the trial, the mouse was allowed to sit on the platform for 15 s before returning to its home cage. Mice that did not find the platform within the time allotted for the trial were guided to the platform. Four trials were performed in 1 day for 5 consecutive days. On day 6, a probe trial was performed with the platform removed. The mouse was placed in a position different from training trials and allowed to swim for 30 s. On day 30, a probe trial was performed on a subset of mice to test long-term memory. Reversal learning was performed on another group of mice by moving the platform to the opposite quadrant. Mice were trained as before for 5 days to learn the new platform location from day 7 to 11, and then probed on day 12 for their memory. Measurements were acquired with Anymaze video tracking software (Stoelting). 12 WT and 13 C-KO mice were used.

### Contextual fear conditioning assay

Mice were placed in a computerized video fear-conditioning system (Med Associates). After 3 min of habituation, either 1 or 5 foot shocks (1 s, 0.75 mA) were delivered with an interval of 1 min. Freezing behavior was monitored during the entire training session. After 1 h, 24 h, and 30 d, mice were returned to the conditioning chamber to test context-evoked freezing behavior for 4 or 6 min. Mice that were conditioned with 5 foot-shocks were tested for freezing behavior in a novel environment with different ceiling, floor texture, and odor, right before the 24 h test. Freezing was defined as absence of movement other than respiration and assessed by automated video tracking software VideoFreeze (Med Associates), and each animal was tested no more than twice.

For the experiments where the mice were exposed to 1 foot shock, 32 WT and 32 C-KO mice were used. Mice were divided into groups that were tested at either 1 h or 24 h after the learning trial and both groups were tested at 30 d. For experiments where the mice were

Author Manuscript Author Manuscript Author Manuscript Author Manuscript

exposed to 5 foot shocks, 58 WT and 63 C-KO mice were used. After the initial training trial, the mice were divided into 4 groups that were tested at different intervals after training: (a) either 1 h only, (b) 24 h only, (c) both 1 h and 24 h, or (d) both 23 h and 24 h after training. Testing at 23 h in a novel environment was not expected to affect the testing at 24 h. The freezing response of mice tested twice in the same training environment was compared with mice tested only once. Since there was no significant difference between the groups, data from the mice that were subjected to repeated testing were combined.

To measure pain sensitivity to foot-shock, gross motor reactivity following the first foot-shock was quantified. The activity burst was quantified as peak activity during the first second following the initial foot-shock, using the Motion Index function (Video Freeze, Med Associates). The activity burst is reported in arbitrary units.

### Cued fear conditioning

Mice (17 WT and 17 C-KO mice) were placed in a near-infrared computerized video fear-conditioning system (Med Associates). After habituating the mice for 3 min, a 20-s tone (conditioned stimulus, CS, 8 kHz, 90 dB) was played and followed by a foot shock (1 s, 0.75 mA). We chose this tone frequency because there was no difference in hearing threshold between WT and C-KO mice, based on the auditory brainstem response tests. The tone and shock were delivered five times at 110 s intervals. Freezing behavior was measured during the entire training period. After 24 h, mice were placed in a chamber with distinct appearance, floor texture, and odor compared to the conditioning chamber, and freezing behavior was monitored for 6 min. After 3 min of habituation (pre-CS), the CS tone was played continuously for 3 min. Freezing was assessed as described for contextual fear conditioning. A different cohort of mice were used for these experiments and the contextual fear conditioning experiments.

### Open field test

Mice (n = 51 WT, 50 C-KO) were placed in an open field apparatus (40 cm W × 40 cm D × 35 cm H, Stoelting) under bright illumination for 10 min. General motor ability (distance traveled and speed) and anxiety-related behavior (time in center space) were recorded using Anymaze video tracking software (Stoelting).

### Light/ dark box test

Mice (n = 47 WT,48 C-KO) were placed in a light/dark box (40 cm W × 40 cm D × 35 cm H, Stoelting) for 10 min. General motor ability (distance traveled and speed) and anxiety-related behavior (time in the light or dark chamber) were recorded using software Anymaze video tracking software (Stoelting).

### Elevated plus maze

The cross-shaped maze had two open and two closed arms (35 cm W × 35 cm L × 15 cm H for each arm), and was elevated 50 cm above the floor (Stoelting). Mice (n = 49 WT, 50 C-KO) were placed in the center facing one of the open arms, and were then allowed to freely explore the maze for 10 min. Time spent in the open and closed arms, entries to the open and

Author Manuscript Author Manuscript Author Manuscript Author Manuscript

closed arms, and general motor activity (distance and speed) were measured with Anymaze video tracking software (Stoelting).

## BrdU staining

Labeling of newly born neurons with 5'-bromo-2-deoxyuridine (BrdU, Sigma-Aldrich) was performed as previously described (Lee et al., 2016). Mice (n = 9 WT,9 C-KO) were given intraperitoneal injections of the thymidine analog bromodeoxyuridine (BrdU, 150 mg/kg/d) once. After 30 d, mice were euthanized by transcardial perfusion with 4% paraformaldehyde in PBS at pH 7.4 (PFA). Brain were dissected and immersed in 4% PFA overnight at C, cryoprotected in 30% sucrose in 1X PBS, and cryosectioned into 40 μm free-floating sections. Sections were blocked with 50% formamide/2× saline-sodium citrate (SSC) at 65°C for 2 h, one wash in for 5 min and in 2 M HCI at 37° C for 30 min. Sections were processed for immunohistochemical staining with mouse monoclonal anti-BrdU (1:100, Roche). The number of BrdU+ cells in the entire dentate gyrus subgranular zone (SGZ) was quantified by counting BrdU+ cells within the SGZ and dentate gyrus in every fifth section throughout the entire hippocampus, and then normalizing for dentate gyrus volume using Nikon Metamorph and NIH ImageJ software with appropriate conversion factors.

## Electrophysiology

Mice (n = 7 WT, 6 C-KO; 2–4 month old males) were anesthetized with a mixture of ketamine, xylazine, and acetopromazine (100, 15, and 5 mg/kg body weight, respectively) and intracardially perfused with ice-cold cutting solution containing (in mM): 28 $NaHCO_3$, 1.25 $NaH_2PO_4$, 2 KCl, 7 $MgCl_2$, 0.5 $CaCl_2$, 7 d-glucose, 220 sucrose, 1 acetic acid, and 3 sodium pyruvate pH 7.4, bubbled with carbogen. The brain was dissected and sectioned into coronal slices (375 μm) with a vibratome (OTS-5000, Electron Microscopy Sciences) in ice-cold cutting solution. After sectioning, the slices were transferred to artificial cerebrospinal fluid (ACSF) containing (in mM): 125 NaCl, 25 $NaHCO_3$, 1.25 $NaH_2PO_4$, 2.5 KCl, 1 $MgCl_2$, 2 $CaCl_2$, 25 D-glucose, pH 7.4. The brain slices were incubated at 34 °C for 30 min in ACSF before allowing to recover for at least 30 min at RT before recording. All chemicals were obtained from Sigma.

For recording, brain slices were mounted into a recording chamber and visualized on an Olympus BX51 microscope with water-immersion 40x objective. Field excitatory postsynaptic potentials (fEPSPs) were recorded with a HEKA (Lambrecht/Pfalz, Germany) EPC 10 amplifier using Patchmaster V2×73.3 (HEKA) on a Windows operating system, with the gain set to Vmon*100. Recording electrodes were filled with standard ACSF, with a pipette resistance of 4–8 mOhm. Stimulating electrodes were standard recording electrodes broken to a tip size of 10–20 μm. Stimuli were applied via DAC control with Patchmaster, using a Digitimer DS3 (Hertfordshire, England) current stimulator. The recording electrode was placed in stratum radiatum of the CA1 region, and a monopolar stimulating electrode in stratum radiatum. Stimulus intensity was adjusted to give an approximately 1 mV fEPSP to monitor the response, and during the potentiating tetanus stimulus intensity was increased by 1.5x. A 1-sec, 100-Hz tetanus was applied twice, with a 20 s interval. All analysis was conducted using custom macros in IGOR (Wavemetrics, Lake Oswego, Oregon) and GraphPad Prism 7.0 (La Jolla, California).

Author Manuscript Author Manuscript Author Manuscript Author Manuscript

### Experimental design and statistical analysis

For all experiments except the electrophysiology experiment, equal numbers of male and female mice were used. Statistical analysis was done with GraphPad Prism software 7 (RRID: SCR_002798) unless noted otherwise. An alpha level of 0.05 was used for all statistical tests. Data were first tested for normality by Shapiro-Wilk normality test. If the data were normally distributed, unpaired *t* test or ANOVA with post hoc Bonferroni' multiple ompari on test was performed where the significant level was set a α/m (m is the number of null hypotheses). This was calculated by Prism GraphPad using the default settings. Otherwise, Mann-Whitney test was performed using the Prism GraphPad default settings where the number of comparisons = number of values in group A × number of values in group B. If the data had different variance tested by *F* te t Welch' correction a performed. For 2-way ANOVA test, the main effects were reported if there was no significant interaction, and post hoc analysis was performed on the main effects that had more than two levels. Otherwise, post hoc tests were performed and simple main effects were reported using adjusted *p* value for multiple comparisons using Bonferroni' multiple test. Prism computes the multiple comparison tests using a pooled error term, which generates large df for multiple comparisons. When there is significant statistic difference, the effective size Cohen's *d* or $\eta^2$ value was reported. For t test, Mann-Whitney, and post-hoc Bonferroni' test Cohen' *d* was calculated by equation $d = (M2 - M1)/\sqrt{((n1-1)SD1^2 + (n2-1)SD2^2)/(n1+n2-2)}$, where M1, M2, n1, n2, SD1 and SD2 are the mean (M), number of samples (n), and standard deviation (SD) of the WT (1) and C-KO (2) mice. For 2 way ANOVA test, $\eta^2$ was calculated using equation $\eta^2 = SS_{effect} / SS_{total}$, where SS is the sum of squares. Error bars represented standard deviation (SD) for scatter plots and standard error of the mean (SEM) for other graphs.

## Results

### Caldendrin is the major CaBP1 splice variant expressed in the hippocampus

Alternative splicing of exons 1 and 2 of CaBP1 gives rise to variants that differ in sequence from the N-terminal to the first EF-hand domain (Fig.1A). C-KO mice were generated using a targeting construct that disrupts expression of all CaBP1 splice variants (Kim et al., 2014). Antibodies recognizing all CaBP1 variants strongly label pyramidal neurons and interneurons in the hippocampus (Kim et al., 2014). By quantitative PCR, caldendrin, which has the longest N-terminal domain (Fig.1A), is the splice variant most highly expressed in mouse brain (Kim et al., 2014). To verify this at the protein level, we performed western blotting of hippocampal lysates of WT and C-KO mice. Consistent with previous detection of caldendrin in western blots of the mouse forebrain (Kim et al., 2014), bands were detected at 33- and 38-kDa in hippocampal lysates of WT but not C-KO mice (Fig.1B). The two proteins are likely products of alternative start sites (Kim et al., 2014). The lack of bands corresponding to the shorter CaBP1 variants (~18- and 27 kDa; Fig.1B) agrees with the overall low levels of their corresponding mRNAs in mouse brain (Kim et al., 2014).

Author Manuscript Author Manuscript Author Manuscript Author Manuscript

## Spatial memory and reversal learning is impaired in C-KO mice

Based on the abundance of CaBP1 in the hippocampus (Laube et al., 2002, Kim et al., 2014), we hypothesized that CaBP1 may play a role in hippocampal-dependent learning and memory. To test this, we compared the performance of WT and C-KO mice in the Barnes maze, which is commonly used to assess spatial learning and memory (Barnes, 1979). In this assay, mice are placed on a circular table with holes equally spaced around the perimeter, one of which contains an escape chamber. Mice were trained for 4 consecutive days to locate the escape chamber based on visual cues around the table. On day 5, mice were then tested for their memory of the location of the hole with the escape chamber removed (Fig. 2A). We evaluated the number of entries into the escape zone (4 cm surrounding the escape hole) and also how much time mice spent in this region (Fig.2B,C). While there was no difference between WT and C-KO female mice in this assay, C-KO males made fewer entries and spent less time within the escape zone compared to WT males (Fig.2B,C). These results suggest a role for CaBP1 in regulating spatial memory of males but not females.

To follow up on this result, we used a second test of spatial learning and memory—the Morris water maze (Morris, 1984). In this assay, mice were trained for 5 days to swim to a hidden platform submerged in a pool of opaque water using visual cues, and then tested on the $6^{th}$ day for their ability to locate the previous placement of the platform, which was removed from the pool. Despite the results on the Barnes maze (Fig.2), there were no sex-specific differences or differences in WT and C-KO mice in the ability to locate the platform in this assay (data not shown). To test whether plasticity of spatial memory might be affected in C-KO mice, we performed a variant of the Morris water maze that tests the ability to extinguish a previous memory while acquiring a new one (Vorhees and Williams, 2006), which is routinely applied in our laboratory (Voorhees et al., 2017). In the reversal learning assay, mice subject to the standard Morris water maze were subsequently trained for an additional 5 days to learn a new location of the platform, and then subjected to another memory test on day 6 (day 12 after the initial training period; Fig.3A). In this more rigorous experimental paradigm, C-KO mice took longer than WT mice to find the platform (Fig.3B) which was not due to any differences in swim speed between C-KO and WT mice (Fig.3C). C-KO mice also made fewer entries (Fig.3D) and spent significantly less time (Fig.3E) in the target zone on the test day. Thus, reversal learning is significantly impaired in the absence of CaBP1.

## Contextual fear conditioning is enhanced in C-KO mice

In addition to its role in spatial memory, the hippocampus also participates in contextual fear conditioning (Phillips and LeDoux, 1992). In this form of associative learning, mice are placed in a novel environment (conditioning stimulus, CS) that they learn to associate with an aversive stimulus, in this case a foot shock (unconditioned stimulus, US). The level of conditioned fear is represented by the amount of time mice spend freezing (Curzon et al., 2009). When only one foot shock was used (Fig. 4A), there was no difference in freezing time between WT and C-KO mice during training (Fig. 4B), or 1h, 24 h, or 30 d after training (Fig.4C–E). To determine whether fear-conditioning might be altered in C-KO mice exposed to a stronger conditioning paradigm, mice were then trained with 5 foot-shocks (Fig.5A). Compared to WT mice, C-KO mice showed significantly increased freezing time

Author Manuscript Author Manuscript Author Manuscript Author Manuscript

during training (Fig.5B), but not 1 h after training (Fig.5C). However 24 h after training, freeze times of C-KO mice were significantly longer than for WT mice (Fig.5D). These results suggested that while short-term fear memory was not affected in C-KO mice, there is enhanced long-term fear memory in C-KO compared to WT mice. When the mice were placed in a novel chamber distinct from the CS chamber 23 h after the training and before the 24 h test, there was no difference in freeze time of WT and C-KO mice (Fig.5E). After the first foot shock the gross motor activity of WT (2528 ± 185 a.u., artificial unit) and C-KO (2519 ± 221 a.u.) was similar (data not shown). This result argues against a role for increased pain sensitivity in the enhanced freezing responses of C-KO mice. Taken together, our findings indicate that C-KO mice exhibit heightened freezing responses that are specific to the context in which the fear memories were acquired.

### Cued fear conditioning is not affected in C-KO mice

To further evaluate if the enhanced freeze time in context fear conditioning is amygdala-dependent, we also analyzed cued fear conditioning, an alternative form of fear condition that also involves the microcircuitry of the central amygdala but does not depend on the hippocampus (Ciocchi et al., 2010). Training consisted of exposing mice to 5 tones (CS) paired with foot-shocks, followed by testing their freeze time in a novel environment with and without presentation of the tone (Fig.6A). There was no difference in freeze time between WT and C-KO mice during the training or the testing (Fig.6B,C). Therefore, the alterations in fear conditioning in C-KO mice are specific for contextual (processed by the hippocampus) and not cued auditory cues.

### C-KO mice exhibit a mild-anxiety phenotype

The greater freezing behavior of C-KO mice during the 5-shock conditioning paradigm (Fig. 5A) may have resulted from greater anxiety in these mice. To test whether C-KO mice exhibit greater anxiety-like behavior, we performed the open field test in which mice are placed in an open chamber. In this test, the time spent along the perimeter and in the center are bidirectionally associated with anxiety. C-KO mice spent slightly but significantly more time around the edges and less time in the center of the chamber (Fig.7A), consistent with greater anxiety in C-KO than WT mice. However, increased anxiety-like behavior was not detected for C-KO mice in other assays. For example, in the light/dark box test, there were no differences in the time spent by WT and C-KO mice in the light or dark chambers (Fig. 7B). Moreover, there were no differences in the time spent by WT and C-KO mice in the open and closed arms of the elevated plus maze (Fig.7C). This distance traveled by C-KO mice was also similar to that of WT mice in all these tests (Fig.7A–C, right panels), suggesting no locomotion defects in C-KO mice. These results suggest that C-KO mice exhibit a mild anxiety phenotype.

### Adult C-KO mice have reduced numbers of newborn hippocampal neurons and impaired hippocampal LTP

In the subgranular zone of the dentate gyrus within the adult hippocampus, the birth of new neurons and their integration into the hippocampal circuitry is thought to be important in the control of anxiety- and fear conditioning behavior (Saxe et al., 2006, Revest et al., 2009, Snyder et al., 2011), as well as spatial memory (Snyder et al., 2005). To determine whether

Author Manuscript Author Manuscript Author Manuscript Author Manuscript

adult neurogenesis and/or neuron survival was altered in C-KO mice, we tracked the number of surviving newborn neurons in WT and C-KO mice using bromodeoxyuridine (BrdU) to label proliferating cells. Thirty days after the BrdU injection, we analyzed the cryosections through the dentate gyrus for BrdU-positive cells (Fig.8A). There was a significant (~40%) reduction in the number of BrdU-labeled cells in C-KO compared to WT mice (Fig.8B,C). Thus, CaBP1 plays a role in augmenting the net magnitude of newborn neurons in the adult hippocampus.

Long-term potentiation (LTP) is a form of synaptic plasticity associated with spatial memory (Lynch, 2004) and contextual fear learning (Huerta et al., 2000, Rampon et al., 2000). To determine whether LTP was altered in C-KO mice, we measured field excitatory potentials (fEPSPs) in the CA1 region of the hippocampus using a classical LTP induction protocol. In WT brain slices, high-frequency tetanic stimulation the Schaffer collateral pathway produced robust LTP, as indicated by the long-lasting increase in slope of the field excitatory postsynaptic potentials (fEPSPs) in the CA1 region of WT hippocampal slices. By contrast, the same paradigm produced little change in fEPSP slope in C-KO slices (Fig. 9). Thus, weak LTP may contribute to the alterations in spatial memory and fear conditioning in C-KO mice.

## Discussion

### CaBP1 contributes to optimal spatial learning

The subtle impairment of spatial learning of C-KO males but not females in the Barnes maze (Fig.2) suggests a sex-specific role of CaBP1 in spatial memory. Male mice perform better than female mice in some spatial memory tasks (Jonasson, 2005, Bettis and Jacobs, 2009), and ovarian hormones impair performance of female rats in the Morris water maze (Snihur et al., 2008) and diminish hippocampal LTP (Bundy et al., 2017). Although sex differences in the expression pattern of CaBP1 in the brain have not been reported, CaBP1 has been implicated in regulating activity- and NMDA receptor- dependent gene transcription (Dieterich et al., 2008). Considering that there are major differences in hippocampal gene expression patterns in males and females (Bundy et al., 2017), it is intriguing to speculate that loss of CaBP1 may compromise the expression of male-specific genes controlling spatial memory. Future analyses comparing sex-specific gene expression differences in the hippocampus of C-KO mice will shed light on this possibility. The lack of sex-specific effect in the other two hippocampal-dependent behavioral tests could also be explained by the level of stress animals encounter, or different brain circuits recruited.

The mild deficit in reversal learning of C-KO mice in the Morris water maze suggests an impairment in cognitive flexibility in that C-KO mice did not adapt their behavior to find the new location of the platform as well as WT mice were able to do (Fig.3). Impaired reversal learning and LTP have been associated with dysregulation of $Ca^{2+}$ signaling, such as in mice with altered expression of $Ca^{2+}$-CaM- stimulated adenylyl cyclases (Zhang et al., 2011, Zhang and Wang, 2013). Moreover, subchronic treatment with psychomimetic drugs cause deficits in reversal learning and significant reductions in hippocampal expression of the $Ca^{2+}$ buffering protein parvalbumin (Zhang and Wang, 2013). Notably, CaBP1 is expressed both in pyramidal neurons and parvalbumin-positive interneurons in the hippocampus (Kim et al.,

Author Manuscript Author Manuscript Author Manuscript Author Manuscript

2014). Thus, CaBP1 may regulate reversal learning through expression in multiple cell-types.

### CaBP1 regulates contextual fear learning, the number of newborn neurons, and LTP

CaBP1 is highly expressed in neurons in the amygdala (Laube et al., 2002), which is a key component of the neural circuitry underlying cued fear conditioning (Phillips and LeDoux, 1992). Nevertheless, C-KO mice did not differ from WT mice in their freezing responses to auditory cues (Fig.6). Thus, the enhanced freezing responses of C-KO mice in response to foot-shocks both during and 24 h after training (Fig.5) were probably not due to a general enhancement in conditioned fear behavior, as shown in similar responses between WT and C-KO mice in cued fear conditioning and the gross motor reactivity following the first shock. Although anxiety is highly correlated with contextual fear conditioning (Ponder et al., 2007), C-KO mice only exhibited modest anxiety-like behavior in the open field test and not others, suggesting a very mild anxiety phenotype (Fig.7). Moreover, when placed in a novel environment after the training period, C-KO and WT mice exhibited similar levels of freezing behavior (Fig.5E). These results suggest that the increased fear responses of C-KO mice are specific to contextual fear learning, and not a consequence of heightened anxiety.

The deficits in newborn neurons and LTP in C-KO mice are consistent with the impairment in spatial memory in these mice (Lynch, 2004, Snyder et al., 2005). At the same time, enhancements in contextual fear learning are generally associated with an increase in LTP (Schuette et al., 2016) (Jacob et al., 2012) and adult neurogenesis (Song et al., 2016, Sun et al., 2016). The apparent incongruence of the contextual fear conditioning and neurogenesis/LTP phenotypes in our C-KO mice may arise from a shift in the neural substrates underlying contextual fear learning. Previous studies suggest that the hippocampus may prevent acquisition of context learning by other regions of the brain. For example, lesions of the dorsal rat hippocampus impair but do not abolish contextual fear learning (Wiltgen et al., 2006). The implication is that other brain areas, such as the prefrontal cortex and amygdala (Rozeske et al., 2015) may compensate for the lack of the hippocampus' contribution to contextual fear encoding. Similarly, the deficiency in hippocampal LTP in C-KO mice may release a brake on these extra-hippocampal circuits, leading to slightly enhanced contextual fear learning compared to WT mice (Fig.5).

### CaBP1: a modulator of neuronal $Ca^{2+}$ signals

The relatively minor effects of CaBP1 knock-down on contextual fear conditioning (Fig.5), spatial memory (Fig.2,3), and anxiety-like behavior (Fig.7) may arise from multiple mechanisms. First, C-KO mice are full knock-outs so CaBP1 expression is silenced in a wide variety of neuronal cell groups and from embryonic stages. Therefore, compensatory changes in cellular signaling pathways and neural circuit function may lead to more modest alterations in behaviors than might be expected in a conditional knockout. Second, CaBP1 may serve primarily to fine-tune rather than trigger or curtail $Ca^{2+}$ signaling pathways. A prime example is the regulation of $Ca_V$ $Ca^{2+}$ channels by CaBP1. CaBP1 strongly inhibits $Ca_V2.1$ P/Q-type channels (Lee et al., 2002), which mediate presynaptic $Ca^{2+}$ signals that trigger neurotransmitter release in many brain regions, including the hippocampus (Wheeler et al., 1994). CaBP1 also prolongs $Ca^{2+}$ currents mediated by $Ca_V1.2$ L-type channels (Zhou

Author Manuscript Author Manuscript Author Manuscript Author Manuscript

et al., 2004, Zhou et al., 2005, Tippens and Lee, 2007). $Ca_V1.2$ is thought to be the dominant L-type calcium channel in the brain (Clark et al., 2003), and mediates somatodendritic $Ca^{2+}$ signals coupled to gene transcription (Ma et al., 2013), LTP and spatial memory (Moosmang et al., 2005), and neurogenesis (De Jesus-Cortes et al., 2016, Temme et al., 2016, Volkening et al., 2017). While presynaptic $Ca_V2.1$ $Ca^{2+}$ signals would be potentiated in C-KO mice, postsynaptic $Ca_V1$ currents would be more transient. Thus, while loss-of function of $Ca_V1$ channels may contribute to the impaired LTP and neurogenesis/neuron survival in C-KO mice, the effects of CaBP1 knock-down on behavior may be mitigated by the gain-of function in presynaptic $Ca_V2.1$ channels. Future studies using conditional knockout of CaBP1 in particular cell-types should clarify the extent to which learning and memory are regulated by CaBP1, as well as the underlying mechanisms.

While this manuscript was under review, Mikhaylova et al. published a characterization of the cellular phenotypes of their own C-KO mouse line {Mikhaylova, 2018 #8477}. They elegantly showed that the longest CaBP1 variant, caldendrin, is needed for cytoskeletal alterations involved in remodeling of dendritic spines. Together with the deficits in newborn neurons that we uncovered in our study (Fig.8), abnormalities in postsynaptic structural plasticity may contribute to the impaired learning/memory and LTP in both their and our C-KO mouse lines. Consistent with their findings, we did not find a robust anxiety phenotype in our C-KO mice (Fig.7). However, our additional behavioral analyses confirm the importance CaBP1 in hippocampal function in that C-KO mice exhibit defects in spatial memory in the Barnes maze (Fig.2) and reversal spatial learning in the Morris water maze (Fig.3), as well as enhanced long-term contextual fear memory (Fig.5). Taken together, our findings corroborate and extend those of Mikhaylova in revealing a key role for CaBP1 in hippocampal-dependent synaptic plasticity and learning and memory.

### Conclusions

Although the cellular and subcellular distributions of CaBP1 have been mapped in the brain of rodents (Laube et al., 2002, Kim et al., 2014) and humans (Bernstein et al., 2003, Bernstein et al., 2007), our findings provide new insights into the neural function of CaBP1 in mice. Using C-KO mice, we show that caldendrin is the major CaBP1 variant expressed in the hippocampus (Fig.1). C-KO mice exhibit mild impairments in spatial memory and reversal learning (Fig.2,3), but enhanced contextual fear conditioning (Fig.5), which may result from reductions in newborn immature neurons and LTP (Fig.8,9). We conclude that CaBP1 is necessary for normal synaptic plasticity and the net magnitude of surviving newborn postnatal hippocampal neurons, which may underlie the behavioral abnormalities in C-KO mice.

## References

Barnes CA. Memory deficits associated with senescence: a neurophysiological and behavioral study in the rat. J Comp Physiol Psychol. 1979; 93:74–104. [PubMed: 221551]

Bernstein HG, Sahin J, Smalla KH, Gundelfinger ED, Bogerts B, Kreutz MR. A reduced number of cortical neurons show increased Caldendrin protein levels in chronic schizophrenia. Schizophr Res. 2007; 96:246–256. [PubMed: 17719205]

Author Manuscript Author Manuscript Author Manuscript Author Manuscript

Bernstein HG, Seidenbecher CI, Smalla KH, Gundelfinger ED, Bogerts B, Kreutz MR. Distribution and cellular localization of caldendrin immunoreactivity in adult human forebrain. J Histochem Cytochem. 2003; 51:1109–1112. [PubMed: 12871994]

Bettis TJ, Jacobs LF. Sex-specific strategies in spatial orientation in C57BL/6J mice. Behav Processes. 2009; 82:249–255. [PubMed: 19622389]

Bundy JL, Vied C, Nowakowski RS. Sex differences in the molecular signature of the developing mouse hippocampus. BMC Genomics. 2017; 18:237. [PubMed: 28302071]

Burgoyne RD, Haynes LP. Understanding the physiological roles of the neuronal calcium sensor proteins. Mol Brain. 2012; 5:2. [PubMed: 22269068]

Ciocchi S, Herry C, Grenier F, Wolff SB, Letzkus JJ, Vlachos I, Ehrlich I, Sprengel R, Deisseroth K, Stadler MB, Muller C, Luthi A. Encoding of conditioned fear in central amygdala inhibitory circuits. Nature. 2010; 468:277–282. [PubMed: 21068837]

Clark NC, Nagano N, Kuenzi FM, Jarolimek W, Huber I, Walter D, Wietzorrek G, Boyce S, Kullmann DM, Striessnig J, Seabrook GR. Neurological phenotype and synaptic function in mice lacking the $Ca_V1.3$ alpha subunit of neuronal L-type voltage-dependent $Ca^{2+}$ channels. Neuroscience. 2003; 120:435–442. [PubMed: 12890513]

Cui G, Meyer AC, Calin-Jageman I, Neef J, Haeseleer F, Moser T, Lee A. $Ca^{2+}$-binding proteins tune $Ca^{2+-}$ feedback to $Ca_V1.3$ channels in auditory hair cells. J Physiol. 2007; 585:791–803. [PubMed: 17947313]

Curzon, P., Rustay, NR., Browman, KE. Cued and Contextual Fear Conditioning for Rodents. In: Buccafusco, JJ., editor. Methods of Behavior Analysis in Neuroscience. Boca Raton (FL): 2009.

De Jesus-Cortes H, Rajadhyaksha AM, Pieper AA. Cacna1c: Protecting young hippocampal neurons in the adult brain. Neurogenesis (Austin). 2016; 3:e1231160. [PubMed: 27900342]

Dieterich DC, Karpova A, Mikhaylova M, Zdobnova I, Konig I, Landwehr M, Kreutz M, Smalla KH, Richter K, Landgraf P, Reissner C, Boeckers TM, Zuschratter W, Spilker C, Seidenbecher CI, Garner CC, Gundelfinger ED, Kreutz MR. Caldendrin-Jacob: a protein liaison that couples NMDA receptor signalling to the nucleus. PLoS biology. 2008; 6:e34. [PubMed: 18303947]

Findeisen F, Minor DL Jr. Structural basis for the differential effects of CaBP1 and calmodulin on Ca(V)1.2 calcium-dependent inactivation. Structure. 2010; 18:1617–1631. [PubMed: 21134641]

Finkler A, Ashery-Padan R, Fromm H. CAMTAs: calmodulin-binding transcription activators from plants to human. FEBS Lett. 2007; 581:3893–3898. [PubMed: 17689537]

Haeseleer F, Imanishi Y, Maeda T, Possin DE, Maeda A, Lee A, Rieke F, Palczewski K. Essential role of $Ca^{2+}$-binding protein 4, a $Ca_V1.4$ channel regulator, in photoreceptor synaptic function. Nat Neurosci. 2004; 7:1079–1087. [PubMed: 15452577]

Haeseleer F, Imanishi Y, Sokal I, Filipek S, Palczewski K. Calcium-binding proteins: intracellular sensors from the calmodulin superfamily. Biochem Biophys Res Commun. 2002; 290:615–623. [PubMed: 11785943]

Haeseleer F, Sokal I, Verlinde CL, Erdjument-Bromage H, Tempst P, Pronin AN, Benovic JL, Fariss RN, Palczewski K. Five members of a novel $Ca^{2+}$-binding protein (CABP) subfamily with similarity to calmodulin. J Biol Chem. 2000; 275:1247–1260. [PubMed: 10625670]

Hardie J, Lee A. Decalmodulation of Cav1 channels by CaBPs. Channels. 2016; 10:33–37. [PubMed: 26155893]

Hell JW. CaMKII: claiming center stage in postsynaptic function and organization. Neuron. 2014; 81:249–265. [PubMed: 24462093]

Huerta PT, Sun LD, Wilson MA, Tonegawa S. Formation of temporal memory requires NMDA receptors within CA1 pyramidal neurons. Neuron. 2000; 25:473–480. [PubMed: 10719900]

Jacob W, Marsch R, Marsicano G, Lutz B, Wotjak CT. Cannabinoid CB1 receptor deficiency increases contextual fear memory under highly aversive conditions and long-term potentiation in vivo. Neurobiol Learn Mem. 2012; 98:47–55. [PubMed: 22579951]

Jonasson Z. Meta-analysis of sex differences in rodent models of learning and memory: a review of behavioral and biological data. Neurosci Biobehav Rev. 2005; 28:811–825. [PubMed: 15642623]

Kawasaki H, Kretsinger RH. Structural and functional diversity of EF-hand proteins: Evolutionary perspectives. Protein Sci. 2017; 26:1898–1920. [PubMed: 28707401]

Author Manuscript Author Manuscript Author Manuscript Author Manuscript

Kim KY, Scholl ES, Liu X, Shepherd A, Haeseleer F, Lee A. Localization and expression of CaBP1/caldendrin in the mouse brain. Neuroscience. 2014; 268:33–47. [PubMed: 24631676]

Laube G, Seidenbecher CI, Richter K, Dieterich DC, Hoffmann B, Landwehr M, Smalla KH, Winter C, Bockers TM, Wolf G, Gundelfinger ED, Kreutz MR. The neuron-specific $Ca^{2+}$-binding protein caldendrin: gene structure, splice isoforms, and expression in the rat central nervous system. Mol Cell Neurosci. 2002; 19:459–475. [PubMed: 11906216]

Lee A, Westenbroek RE, Haeseleer F, Palczewski K, Scheuer T, Catterall WA. Differential modulation of $Ca_V2.1$ channels by calmodulin and $Ca^{2+}$-binding protein 1. Nat Neurosci. 2002; 5:210–217. [PubMed: 11865310]

Lee AS, De Jesus-Cortes H, Kabir ZD, Knobbe W, Orr M, Burgdorf C, Huntington P, McDaniel L, Britt JK, Hoffmann F, Brat DJ, Rajadhyaksha AM, Pieper AA. The Neuropsychiatric Disease-Associated Gene cacna1c Mediates Survival of Young Hippocampal Neurons. eNeuro. 2016; 3

Liu X, Kerov V, Haeseleer F, Majumder A, Artemyev N, Baker SA, Lee A. Dysregulation of $Ca_V1.4$ channels disrupts the maturation of photoreceptor synaptic ribbons in congenital stationary night blindness type 2. Channels. 2013; 7:514–523. [PubMed: 24064553]

Lynch MA. Long-term potentiation and memory. Physiol Rev. 2004; 84:87–136. [PubMed: 14715912]

Ma H, Cohen S, Li B, Tsien RW. Exploring the dominant role of Cav1 channels in signalling to the nucleus. Bioscience reports. 2013; 33:97–101.

Moosmang S, Haider N, Klugbauer N, Adelsberger H, Langwieser N, Muller J, Stiess M, Marais E, Schulla V, Lacinova L, Goebbels S, Nave KA, Storm DR, Hofmann F, Kleppisch T. Role of hippocampal $Ca_V1.2$ $Ca^{2+}$ channels in NMDA receptor-independent synaptic plasticity and spatial memory. J Neurosci. 2005; 25:9883–9892. [PubMed: 16251435]

Morris R. Developments of a water-maze procedure for studying spatial learning in the rat. J Neurosci Methods. 1984; 11:47–60. [PubMed: 6471907]

Oz S, Benmocha A, Sasson Y, Sachyani D, Almagor L, Lee A, Hirsch JA, Dascal N. Competitive and non-competitive regulation of calcium-dependent inactivation in CaV1.2 L-type $Ca^{2+}$ channels by calmodulin and $Ca^{2+}$-binding protein 1. J Biol Chem. 2013; 288:12680–12691. [PubMed: 23530039]

Palmer CL, Lim W, Hastie PG, Toward M, Korolchuk VI, Burbidge SA, Banting G, Collingridge GL, Isaac JT, Henley JM. Hippocalcin functions as a calcium sensor in hippocampal LTD. Neuron. 2005; 47:487–494. [PubMed: 16102532]

Phillips RG, LeDoux JE. Differential contribution of amygdala and hippocampus to cued and contextual fear conditioning. Behav Neurosci. 1992; 106:274–285. [PubMed: 1590953]

Picher MM, Gehrt A, Meese S, Ivanovic A, Predoehl F, Jung S, Schrauwen I, Dragonetti AG, Colombo R, Van Camp G, Strenzke N, Moser T. Ca2+-binding protein 2 inhibits Ca2+-channel inactivation in mouse inner hair cells. Proc Natl Acad Sci U S A. 2017; 114:E1717–E1726. [PubMed: 28183797]

Ponder CA, Kliethermes CL, Drew MR, Muller J, Das K, Risbrough VB, Crabbe JC, Gilliam TC, Palmer AA. Selection for contextual fear conditioning affects anxiety-like behaviors and gene expression. Genes Brain Behav. 2007; 6:736–749. [PubMed: 17309658]

Rampon C, Tang YP, Goodhouse J, Shimizu E, Kyin M, Tsien JZ. Enrichment induces structural changes and recovery from nonspatial memory deficits in CA1 NMDAR1-knockout mice. Nat Neurosci. 2000; 3:238–244. [PubMed: 10700255]

Revest JM, Dupret D, Koehl M, Funk-Reiter C, Grosjean N, Piazza PV, Abrous DN. Adult hippocampal neurogenesis is involved in anxiety-related behaviors. Mol Psychiatry. 2009; 14:959–967. [PubMed: 19255582]

Rieke F, Lee A, Haeseleer F. Characterization of Ca2+-binding protein 5 knockout mouse retina. Invest Ophthalmol Vis Sci. 2008; 49:5126–5135. [PubMed: 18586882]

Rozeske RR, Valerio S, Chaudun F, Herry C. Prefrontal neuronal circuits of contextual fear conditioning. Genes Brain Behav. 2015; 14:22–36. [PubMed: 25287656]

Saab BJ, Georgiou J, Nath A, Lee FJ, Wang M, Michalon A, Liu F, Mansuy IM, Roder JC. NCS-1 in the dentate gyrus promotes exploration, synaptic plasticity, and rapid acquisition of spatial memory. Neuron. 2009; 63:643–656. [PubMed: 19755107]

Author Manuscript Author Manuscript Author Manuscript Author Manuscript

Saimi Y, Kung C. Calmodulin as an ion channel subunit. Annu Rev Physiol. 2002; 64:289–311. [PubMed: 11826271]

Saxe MD, Battaglia F, Wang JW, Malleret G, David DJ, Monckton JE, Garcia AD, Sofroniew MV, Kandel ER, Santarelli L, Hen R, Drew MR. Ablation of hippocampal neurogenesis impairs contextual fear conditioning and synaptic plasticity in the dentate gyrus. Proc Natl Acad Sci U S A. 2006; 103:17501–17506. [PubMed: 17088541]

Schrauwen I, Helfmann S, Inagaki A, Predoehl F, Tabatabaiefar MA, Picher MM, Sommen M, Seco CZ, Oostrik J, Kremer H, Dheedene A, Claes C, Fransen E, Chaleshtori MH, Coucke P, Lee A, Moser T, Van Camp G. A mutation in CABP2, expressed in cochlear hair cells, causes autosomal-recessive hearing impairment. Am J Hum Genet. 2012; 91:636–645. [PubMed: 22981119]

Schuette SR, Fernandez-Fernandez D, Lamla T, Rosenbrock H, Hobson S. Overexpression of Protein Kinase Mzeta in the Hippocampus Enhances Long-Term Potentiation and Long-Term Contextual But Not Cued Fear Memory in Rats. J Neurosci. 2016; 36:4313–4324. [PubMed: 27076427]

Sinha R, Lee A, Rieke F, Haeseleer F. Lack of CaBP1/Caldendrin or CaBP2 Leads to Altered Ganglion Cell Responses. eNeuro. 2016; 3

Snihur AW, Hampson E, Cain DP. Estradiol and corticosterone independently impair spatial navigation in the Morris water maze in adult female rats. Behav Brain Res. 2008; 187:56–66. [PubMed: 17913254]

Snyder JS, Hong NS, McDonald RJ, Wojtowicz JM. A role for adult neurogenesis in spatial long-term memory. Neuroscience. 2005; 130:843–852. [PubMed: 15652983]

Snyder JS, Soumier A, Brewer M, Pickel J, Cameron HA. Adult hippocampal neurogenesis buffers stress responses and depressive behaviour. Nature. 2011; 476:458–461. [PubMed: 21814201]

Song NN, Jia YF, Zhang L, Zhang Q, Huang Y, Liu XZ, Hu L, Lan W, Chen L, Lesch KP, Chen X, Xu L, Ding YQ. Reducing central serotonin in adulthood promotes hippocampal neurogenesis. Sci Rep. 2016; 6:20338. [PubMed: 26839004]

Sun Y, Hong F, Zhang L, Feng L. The sphingosine-1-phosphate analogue, FTY-720, promotes the proliferation of embryonic neural stem cells, enhances hippocampal neurogenesis and learning and memory abilities in adult mice. Br J Pharmacol. 2016; 173:2793–2807. [PubMed: 27429358]

Temme SJ, Bell RZ, Fisher GL, Murphy GG. Deletion of the Mouse Homolog of CACNA1C Disrupts Discrete Forms of Hippocampal-Dependent Memory and Neurogenesis within the Dentate Gyrus. eNeuro. 2016; 3

Tippens AL, Lee A. Caldendrin: a neuron-specific modulator of $Ca_v1.2$ (L-type) $Ca^{2+}$ channels. J Biol Chem. 2007; 282:8464–8473. [PubMed: 17224447]

Volkening B, Schonig K, Kronenberg G, Bartsch D, Weber T. Deletion of psychiatric risk gene Cacna1c impairs hippocampal neurogenesis in cell-autonomous fashion. Glia. 2017; 65:817–827. [PubMed: 28230278]

Voorhees JR, Remy MT, Cintrón-Pérez CJ, El Rass E, Khan MC, Dutca LM, Yin TC, McDaniel LN, Williams NS, Brat DJ, Pieper AA. (-)-P7C3-S243 protects a rat model of Alzheimer's disease from neuropsychiatric deficits and neurodegeneration without altering amyloid deposition or reactive glia. Biological Psychiatry. 2017 Nov 6. pii: S0006-3223(17)32145-5.

Vorhees CV, Williams MT. Morris water maze: procedures for assessing spatial and related forms of learning and memory. Nat Protoc. 2006; 1:848–858. [PubMed: 17406317]

Wheeler DB, Randall A, Tsien RW. Roles of N-type and Q-type $Ca^{2+}$ channels in supporting hippocampal synaptic transmission. Science. 1994; 264:107–111. [PubMed: 7832825]

Wiltgen BJ, Sanders MJ, Anagnostaras SG, Sage JR, Fanselow MS. Context fear learning in the absence of the hippocampus. J Neurosci. 2006; 26:5484–5491. [PubMed: 16707800]

Yang T, Scholl ES, Pan N, Fritzsch B, Haeseleer F, Lee A. Expression and Localization of CaBP Ca2+ Binding Proteins in the Mouse Cochlea. PLoS One. 2016; 11:e0147495. [PubMed: 26809054]

Yin TC, Britt JK, De Jesus-Cortes H, Lu Y, Genova RM, Khan MZ, Voorhees JR, Shao J, Katzman AC, Huntington PJ, Wassink C, McDaniel L, Newell EA, Dutca LM, Naidoo J, Cui H, Bassuk AG, Harper MM, McKnight SL, Ready JM, Pieper AA. P7C3 neuroprotective chemicals block axonal degeneration and preserve function after traumatic brain injury. Cell rep. 2014; 8:1731–1740. [PubMed: 25220467]

Author Manuscript Author Manuscript Author Manuscript Author Manuscript

Zhang M, Storm DR, Wang H. Bidirectional synaptic plasticity and spatial memory flexibility require Ca2+-stimulated adenylyl cyclases. J Neurosci. 2011; 31:10174–10183. [PubMed: 21752993]

Zhang M, Wang H. Mice overexpressing type 1 adenylyl cyclase show enhanced spatial memory flexibility in the absence of intact synaptic long-term depression. Learn Mem. 2013; 20:352–357. [PubMed: 23772089]

Zhou H, Kim SA, Kirk EA, Tippens AL, Sun H, Haeseleer F, Lee A. $Ca^{2+}$-binding protein-1 facilitates and forms a postsynaptic complex with $Ca_V1.2$ (L-type) $Ca^{2+}$ channels. J Neurosci. 2004; 24:4698–4708. [PubMed: 15140941]

Zhou H, Yu K, McCoy KL, Lee A. Molecular mechanism for divergent regulation of $Ca_V1.2$ $Ca^{2+}$ channels by calmodulin and $Ca^{2+}$-binding protein-1. J Biol Chem. 2005; 280:29612–29619. [PubMed: 15980432]

Author Manuscript Author Manuscript Author Manuscript Author Manuscript

## Highlights

- CaBP1 regulates contextual fear conditioning
- CaBP1 is required for hippocampal long-term potentiation
- CaBP1 enhances enhances the number of adult-born hippocampal neurons

Author Manuscript Author Manuscript Author Manuscript Author Manuscript

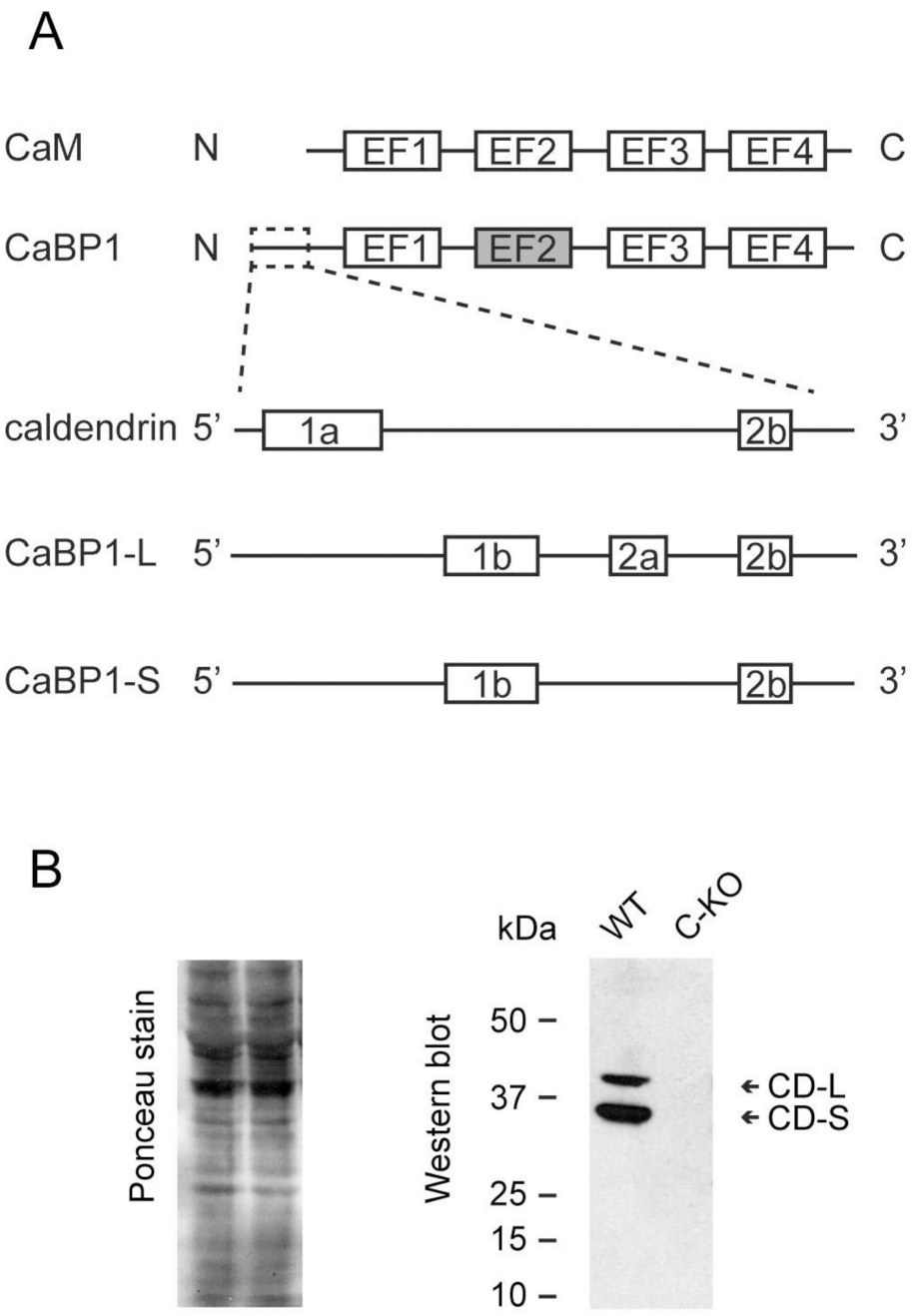


**Figure 1. Caldendrin is the CaBP1 splice variant expressed in the hippocampus**

(A) Schematic showing CaBP1 splice variants. Boxes indicate alternatively spliced exons (numbered) and EF-hand domains. Grey box represents non-functional EF-hand 2. (B) Western blots of hippocampal lysates from WT and C-KO mice probed with antibodies recognizing all CaBP1 splice variants. Two bands corresponding to different caldendrin variants are detected in WT but not C-KO lysates.

Author Manuscript Author Manuscript Author Manuscript Author Manuscript

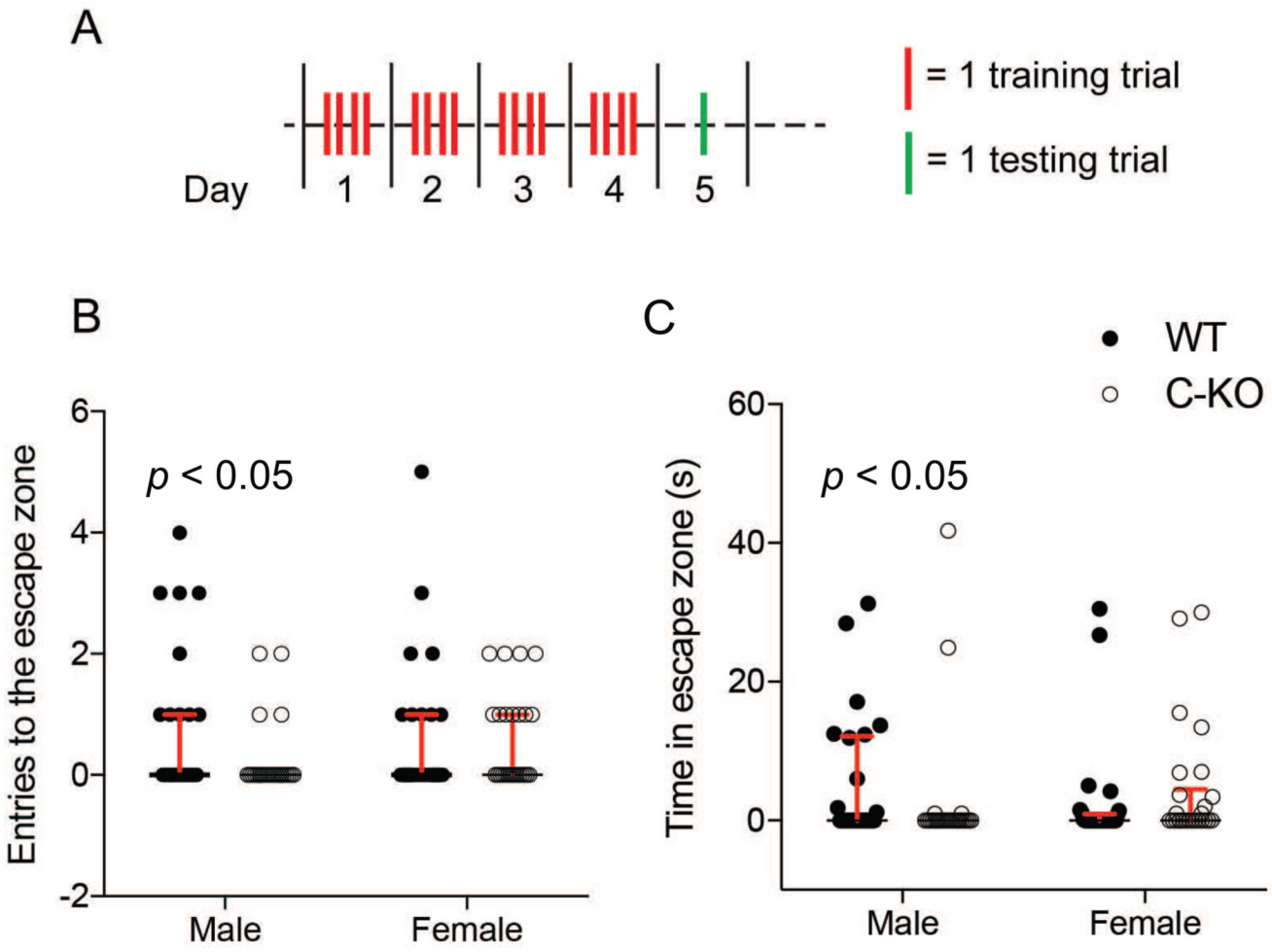


**Figure 2. Male C-KO mice show impaired spatial learning and memory in the Barnes maze**

(A) Experimental paradigm. Mice were trained for 4 days (4 trials/day) to locate the escape zone according to visual cues, and tested on day 5 for the number of entries (B) and time spent (C) in the escape zone. *p* values are shown for the indicated comparisons by Mann-Whitney test ($U(25, 26) = 241$, $p < 0.05$, $d = 0.59$ in *B* and $U(25, 26) = 243$, $p < 0.05$, $d = 0.31$ in *C*). Bars represent median ± interquartile range.

Author Manuscript Author Manuscript Author Manuscript Author Manuscript

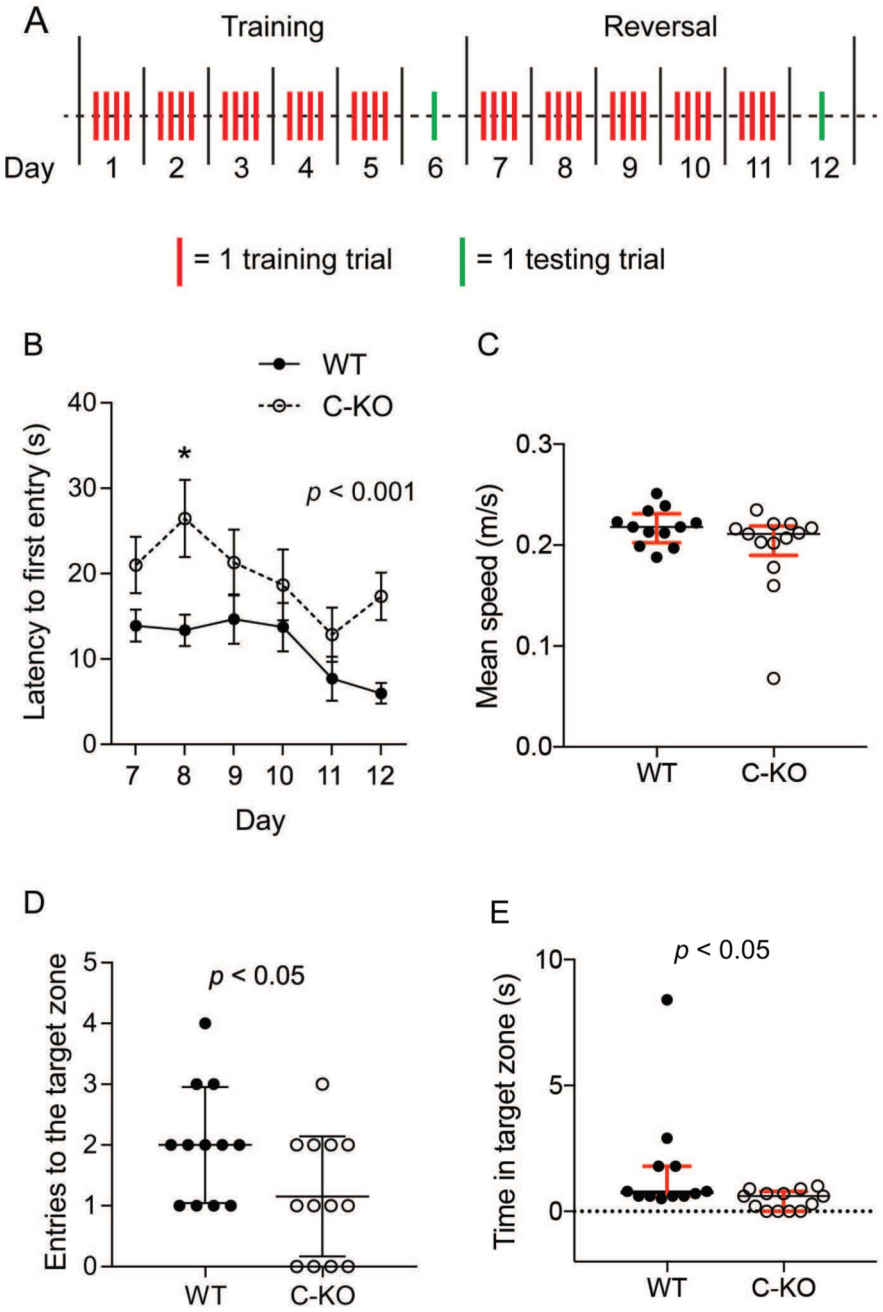


**Figure 3. Reversal spatial learning is impaired in C-KO mice in the Morris water maze**

(A) Experimental paradigm. Mice were trained for 5 days (4 trials/day) to swim to a hidden platform The location of the platform was moved the opposite quadrant, and mice trained for another 5 days to find the platform which was tested 1 day after training. (B) The latency to find the escape platform during reversal training was compared by 2-way ANOVA, $F(1,138) = 19.91$, $p < 0.001$, $\eta^2 = 0.11$, between WT and C-KO; *, $t(138) = 2.965$, $p < 0.05$, $d = 1.06$, by post hoc Bonferroni test. Points represent mean ± SEM. (C) There was no significant difference in the mean swimming speed of WT and C-KO mice ($U(12,13) = 49.50$, $p > 0.05$, by Mann-Whitney test ). (D,E) During the probe trial 1 day after the training, C-KO mice

made significantly less entries (D: $t(23) = 2.176$, $p < 0.05$, $d = 0.47$, by unpaired t-test) and spent less time (E: $U(12,13) = 41$, $p < 0.05$, $d = 0.76$, by Mann-Whitney test) in the target zone compared to WT mice. In *B-E*, n = 12 WT and 13 C-KO mice. Bars represent median ± interquartile range in *C,E*, and mean ± SD in *D*.

Author Manuscript Author Manuscript Author Manuscript Author Manuscript

Author Manuscript Author Manuscript Author Manuscript Author Manuscript

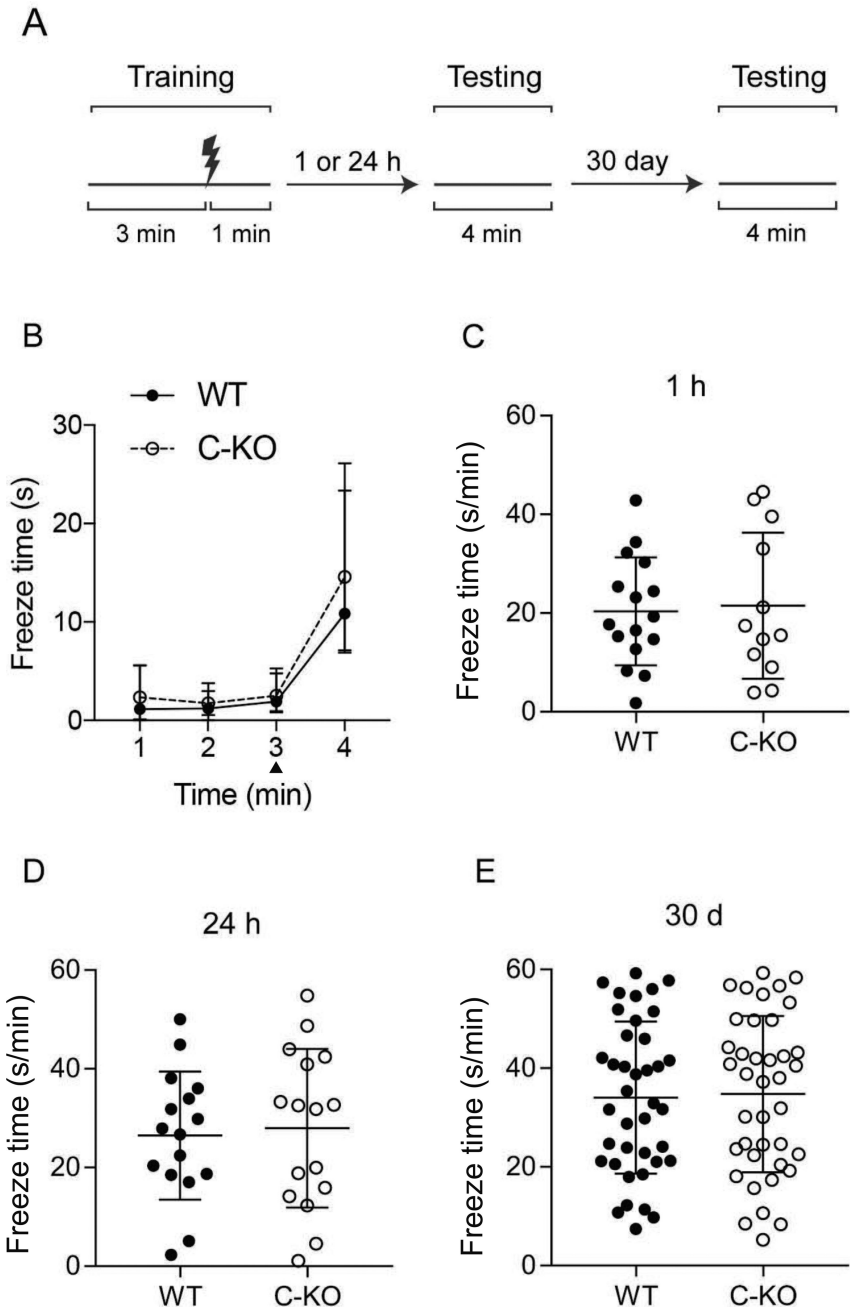


**Figure 4. Contextual fear conditioning is normal with one training trial in C-KO**

(A) Experimental paradigm. Mice were placed in training chamber and after 3 min were exposed to a foot-shock. The mice were kept in the chamber for another 1 min. After the training trial (1 h or 24 h), the mice were exposed to the same training chamber for 4 min. After 30 days, all the mice were exposed to the same training chamber again for 4 min. (B) The freeze time (median ± interquartile range) of mice (n= 32 WT, 32 C-KO) over the course of 4 min training is shown. ▲ foot-shock. There was no significant difference between WT (n =32) and C-KO (n = 32) mice, $F(1,248) = 1.644$, $p = 0.20$ by 2-way ANOVA on ranks. (C–E) Mice were tested for their freeze time 1 h (C) or 24 h (D) after the training

Author Manuscript Author Manuscript Author Manuscript Author Manuscript

(B), and 30 days afterwards (E). The mice were kept in the chamber for a total duration of 4 min, and the average freeze time per min was calculated. There was no significant difference between WT and C-KO mice 1 h (C; $t(26) = 0.23$, n = 16 WT, 12 C-KO); 24 h (D; $t(30) = 0.30$, n = 16 WT, 16 C-KO), or 30 d (E; $t(76) = 0.21$, n = 32 WT, 32 C-KO), each by unpaired t-test. In *C–E*, bars represent mean ± SD.

Author Manuscript Author Manuscript Author Manuscript Author Manuscript

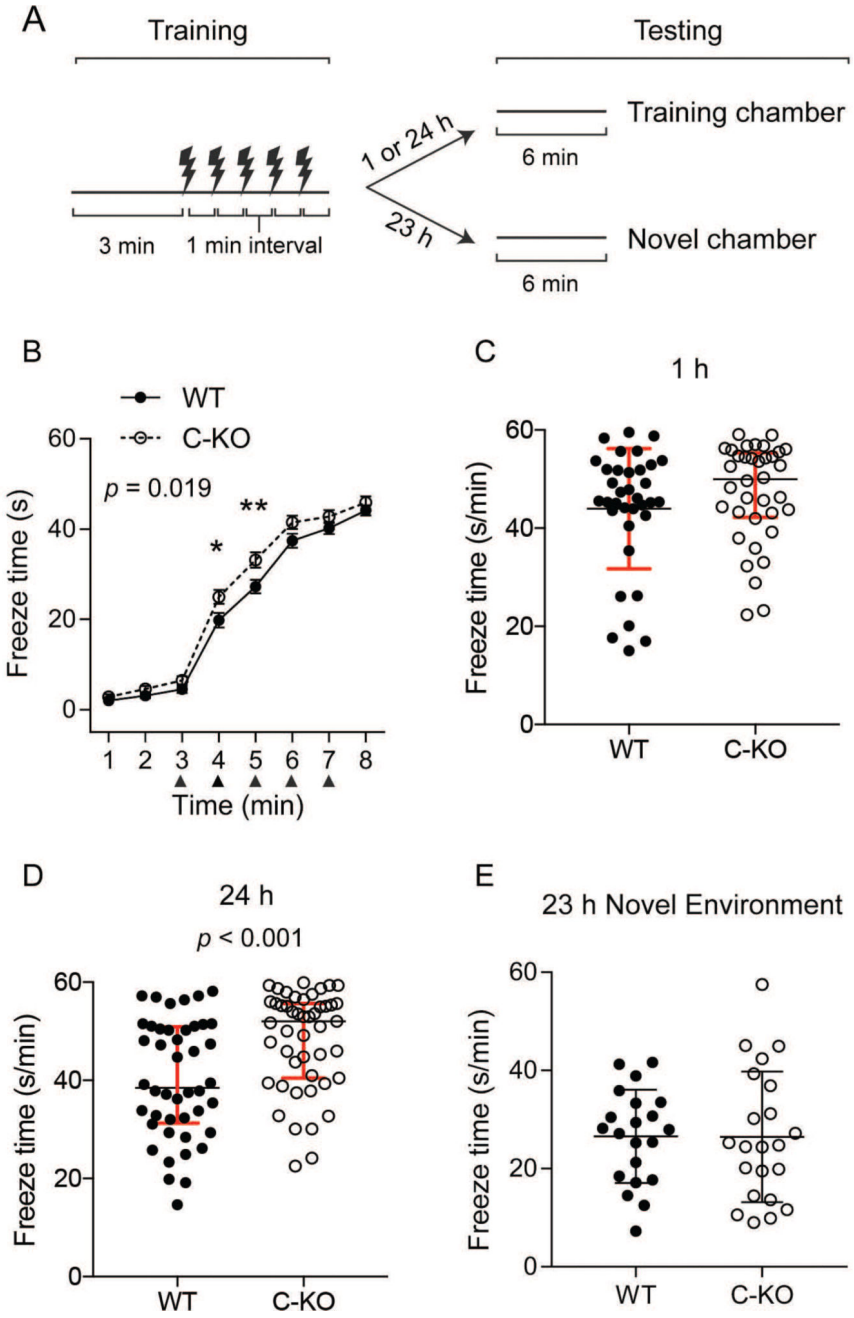


**Figure 5. Long-term fear memory is enhanced in C-KO with stronger conditioning paradigm**

(A) Experimental paradigm. Mice were placed in chamber and after 3 min were exposed to 5 foot-shocks at 1 min intervals. The mice were kept in the chamber for another 1 min before returning them to the home cage. After the training trial (1 h or 24 h), the mice were exposed to the same training chamber for 6 min; 23 h after the training, the mice were exposed to a different chamber for 6 min. (B) The freeze time of mice over the course of 8 min training was shown. ▲ foot-shock. The freeze time in C-KO mice was significantly increased ($F(1,117) = 5.674$, $p < 0.05$, $\eta^2 = 0.01$, by repeated measures 2-way ANOVA; *, $t(936) = 2.958$, $p < 0.05$, $d = 0.42$; $t(936) = 3.379$, $p < 0.01$, $d = 0.47$, by post hoc Bonferroni test, n =

Author Manuscript Author Manuscript Author Manuscript Author Manuscript

58 WT, 63 C-KO mice). Points represent mean ± SEM. (C–E) The mice were kept in the chamber for a total duration of 6 min, and the average freeze time per minute was calculated. While there was no difference in the freeze time of WT and C-KO mice 1 h after the training in the same training chamber (C; U(35,36), $p > 0.05$, n = 35 WT, 36 C-KO mice), the difference was significant at 24 h (D; $U(44,47)$ $p < 0.001$, $d = 0.73$, n = 44 WT, 47 C-KO mice), by Mann-Whitney test. There was no significant difference in WT and C-KO mice 23 h after the training in a different chamber (E; t(41) = 0.03, $p > 0.05$, by unpaired t-test, n = 21 WT, 22 C-KO mice). Bars represent median ± interquartile range in *C,D*, and mean ± SD in *E*.

Author Manuscript Author Manuscript Author Manuscript Author Manuscript

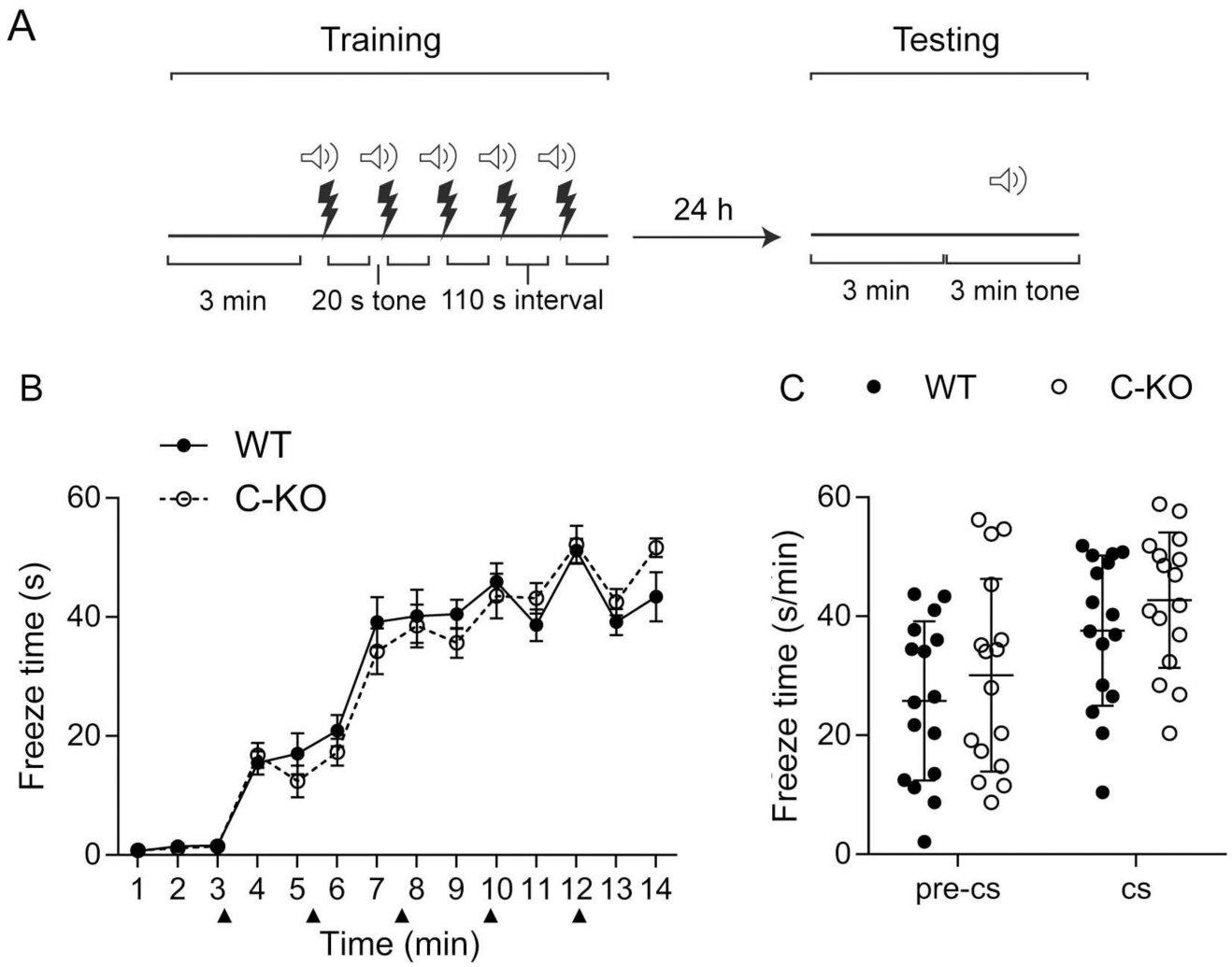


**Figure 6. Cued fear learning and memory is normal in C-KO mice**

(A) Experimental paradigm. WT and C-KO mice were subjected to cued fear conditioning. After 3 min of free-exploring time, mice were exposed to 5 paired tone and foot shocks at 110 s intervals. Mice were tested for their freeze time 24 h after the training in a novel chamber for a total of 6 min, with the tone played in the second half. (B) The freeze time of mice over the course of 14 min is ho n. ▲, foot-shock. Points represent mean ± SEM. The freeze time in C-KO mice (n = 15) was not different from WT (n = 15) mice ($F(1,28) = 0.013$, $p > 0.05$ by repeated measures 2-way ANOVA). (C) Freeze times were tested 24 h later in a novel environment. After 3 min, the tone (cs) was applied for 3 min and the average freeze time over either 3 min interval (pre-cs, cs) was shown. Bars represent mean ± SD. There was no difference in freeze time between WT (n = 16) and C-KO (n = 16) mice ($F(1,30) = 1.306$, $p > 0.05$, by repeated measures 2-way ANOVA). In *C*, equal numbers females and males were used per genotype.

Author Manuscript Author Manuscript Author Manuscript Author Manuscript

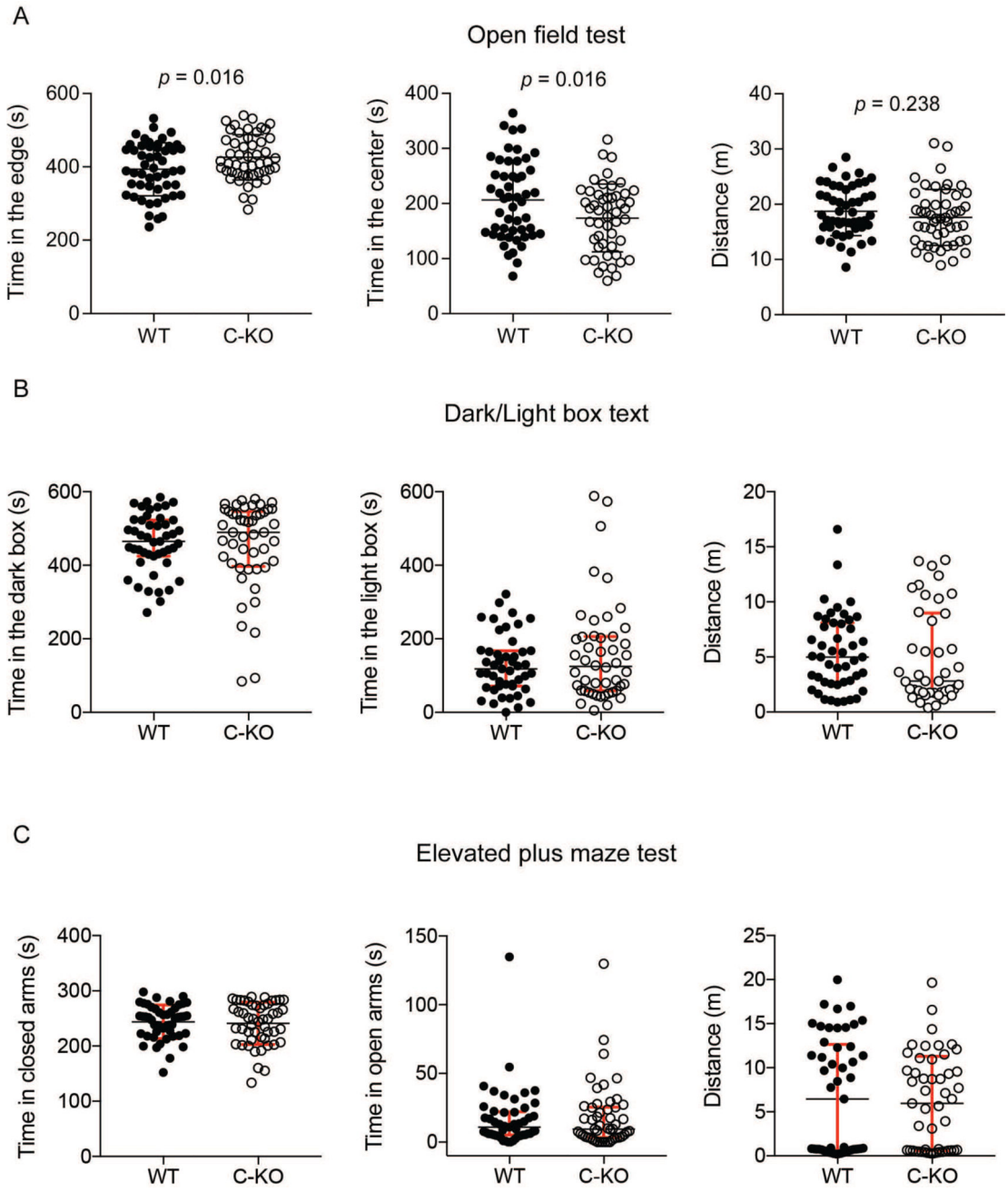


**Figure 7. C-KO mice show moderately increased anxiety-like behavior in the open field test**

(A) In open field tests, mice were placed in testing chamber and time spent around the edges and center, and distance traveled are shown. Compared to WT mice (n = 51), C-KO (n = 51) mice spent significantly more time around the edges ($t(99) = 2.5$, $p < 0.05$, $d = 0.49$) and less time in the center ($t(99) = 2.5$, $p < 0.05$, $d = 0.49$), by unpaired t-test. There was no difference in total distance traveled ($t(99) = 1.2$, $p > 0.05$ by unpaired t-test). Bars represent mean ± SD. (B) In the dark/light box test, mice were placed in testing chamber and time spent in either dark or light box, and distance traveled are shown. $p$ values for the indicated comparisons are shown by Mann-Whitney test. There was no difference between WT and C-

Author Manuscript Author Manuscript Author Manuscript Author Manuscript

KO mice in the time spent in dark box (U(47,48) = 1039, $p > 0.05$), the time spent in the light box (U(47,48) = 1066, $p > 0.05$), or the total distance traveled (U(47,42)= 1039, $p > 0.05$), by Mann-Whitney test. (C) In the elevated plus maze test, mice were placed in maze and time spent in the open and closed arms, and distance traveled are shown. There was no difference between WT and C-KO mice in the time spent in closed arms (U(49,50) = 1219, $p > 0.05$), the time spent in open arms (U(49,50) = 1182, $p > 0.05$), or the total distance traveled (U(49,50) = 1080, $p > 0.05$), by Mann-Whitney test. In *B,C*, bars represent median ± interquartile range.

Author Manuscript Author Manuscript Author Manuscript Author Manuscript

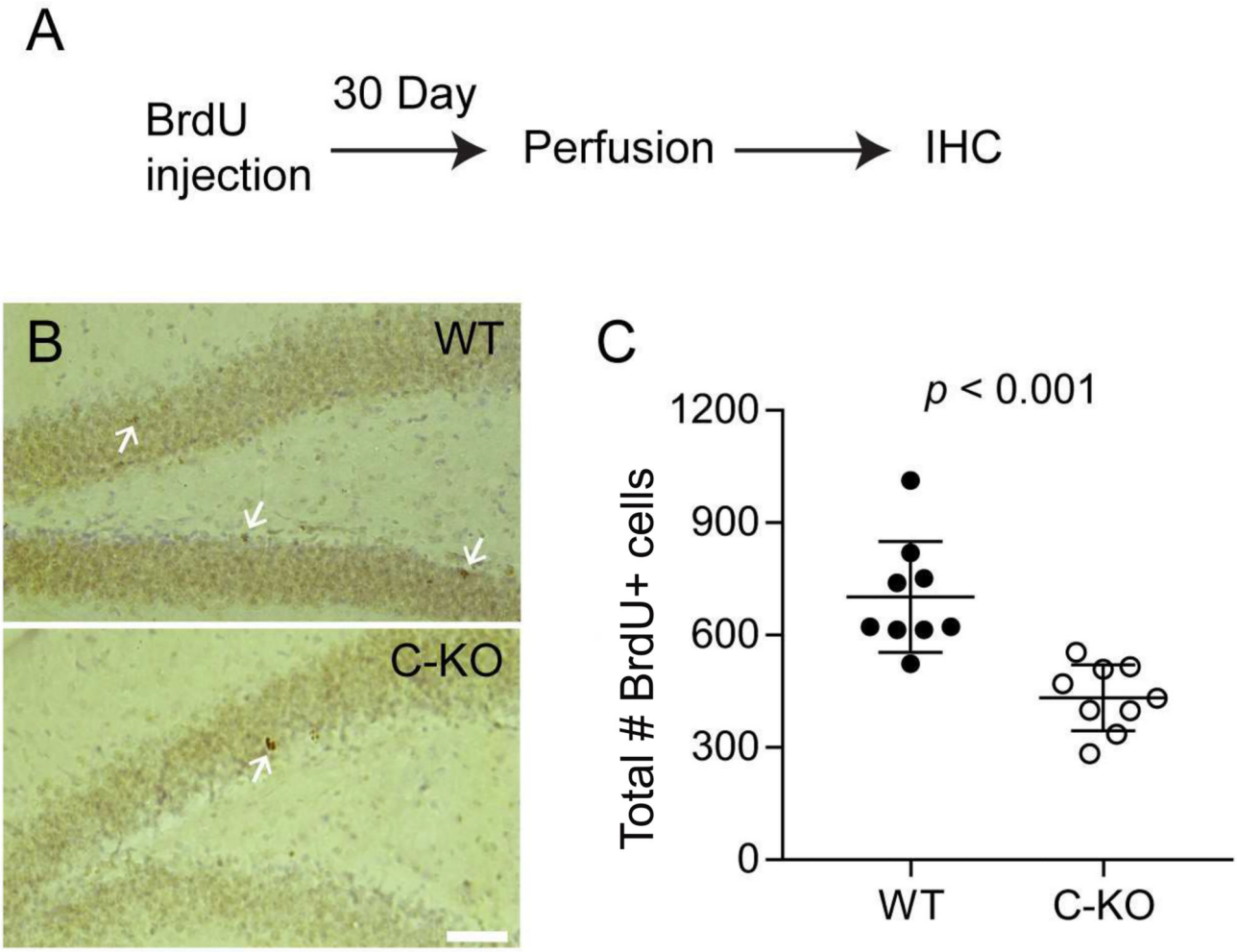


**Figure 8. The number of adult-born neurons is reduced in the hippocampus of C-KO mice**

(A) Experimental paradigm. IHC, immunohistochemistry for BrdU+ cells. (B) Representative images of the dentate gyrus from WT (A) and C-KO (B) hippocampus. Arrows, BrdU+ cells. Scale bar, 50 μm. (C) Quantification of the total number (#) of BrdU+ cells from the entire dentate gyrus subgranular zone in each mouse. Compared to WT mice (n = 9), there was a significant decrease in the number of BrdU+ cells in C-KO (n = 9) mice ($t(16) = 4.694$, $p < 0.001$, $d = 2.25$, by Welch-corrected t-test). Bars represent mean ± SD.

Author Manuscript Author Manuscript Author Manuscript Author Manuscript

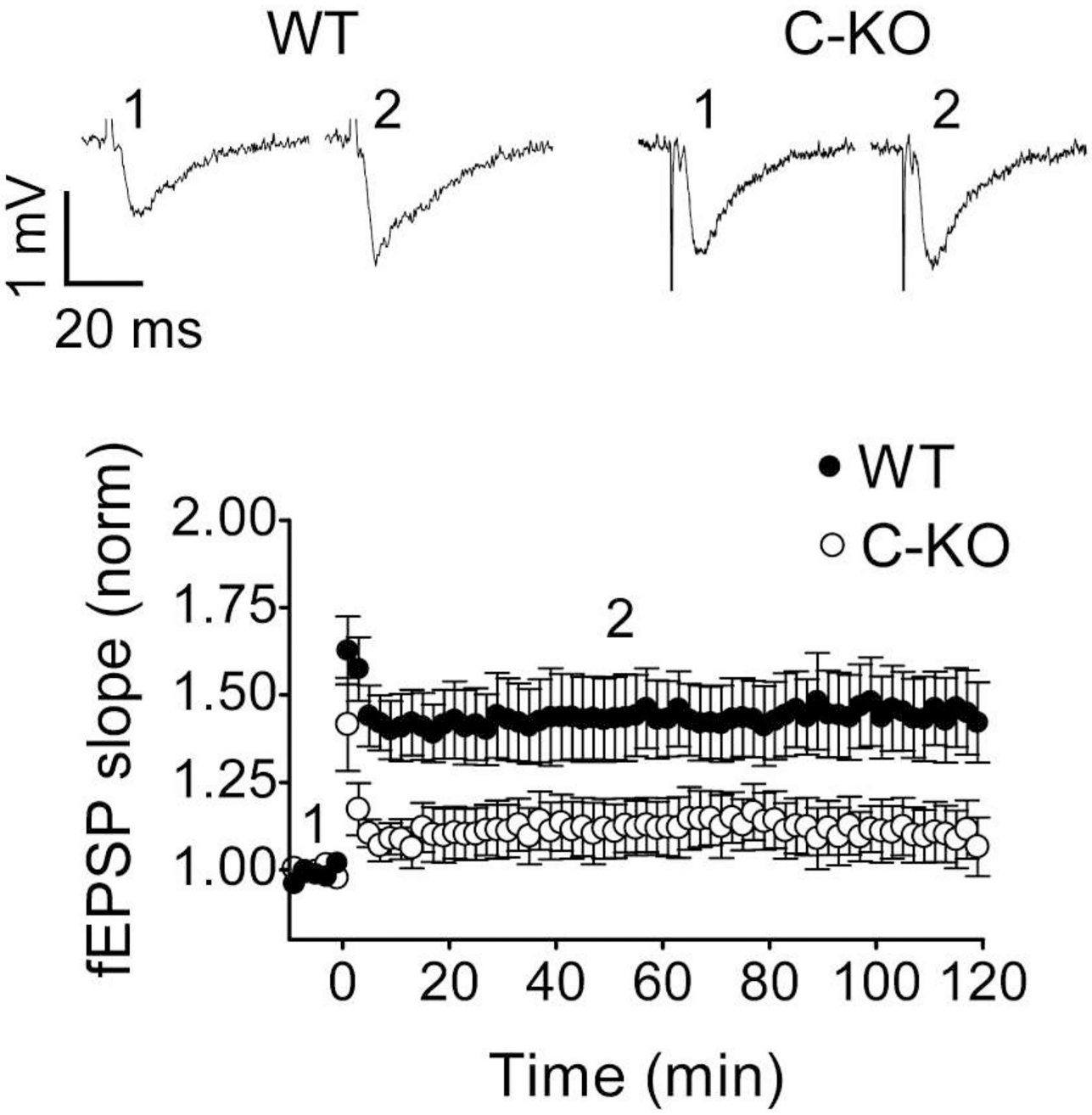


**Figure 9. LTP is impaired at CA3-CA1 synapses in the hippocampus of C-KO mice**

fEPSPs were measured in the stratum radiatum of the CA1 region following stimulation of Schaeffer collaterals in the stratum radiatum. To induce LTP, a 1-sec, 100-Hz tetanic stimulation was applied twice, with a 20 sec interval. *Top*, exemplar traces corresponding to pre-tetanus (1) and post-tetanus (2) fEPSPs. *Bottom*, The slope of fEPSPs normalized to the initial pre-tetanus fEPSP was plotted against time. There was a significant decrease in normalized fEPSP slope at time = 20–30 min ($F(1,11) = 5.831$, $p < 0.05$, $\eta^2 = 0.31$, by 2-way

ANOVA repeated measures) in brain slices from CaBP1 KO (n=6) mice than from WT (n=7) mice. Points represent mean ± SEM.

Author Manuscript Author Manuscript Author Manuscript Author Manuscript